CHEMICAL ENGINEERING TRANSACTIONS
VOL. 104, 2023
A publication of AIDIC
The Italian Association of Chemical Engineering
Online at www.cetjournal.it
Guest Editors: Sabrina Copelli, Ernesto Salzano

ISBN 979-12-81206-06-9; **ISSN** 2283-9216
DOI: 10.3303/CET23104012

Turbulent Ignition Regimes in 20 L Explosion Vessel: CFD Simulations

Maria Portarapillo, Almerinda Di Benedetto

Department of Chemical, Materials and Production Engineering, University of Naples Federico II, P.le Tecchio 80, 80125, Naples, Italy
Maria.portarapillo@unina.it

The understanding of the ignition process is important for many practical and fundamental applications including safety, chemical conversion, flame stabilization, and internal combustion engines operation. The ignition process can be influenced by many factors, including the pre-ignition turbulence level. Turbulence can generally be generated intentionally by the introduction of gases into the combustion chamber, but it can also occur unintentionally, for example by a sudden release of gases into the atmosphere as a result of an accident. Through the small scale 20 L CFD simulations of the ignition process of a stoichiometric methane-air mixture at different ignition energies and levels of turbulence, the present work aims to create a simple operational map that correlates the ignition energy with the degree of turbulence to understand in which areas flame propagation is successful and in which it is not. Such a tool may be useful both for evaluating the operation of internal combustion engines, where ignition and flame propagation are desired phenomena, and for a preliminary assessment of the risk and probability of ignition. This approach may also be applied in the future to other gaseous (as in the case of hydrogen), liquid, or solid systems.

1. Introduction

In chemical industrial processes, many accidents are due to the explosions of flammable mixtures causing serious damage to people and the environment. Measures for prevention and damage limitation are based on knowledge of the parameters that fully characterize the flammability and explosive properties of flammable mixtures. The minimum ignition energy is one of the key factors in both the design of ignition means and the prevention of explosion hazards. There are several experimental data on minimum ignition energies relative to the main combustible gases (such as hydrogen, hydrocarbons etc.), liquids and dust, often determined by experiments with electric sparks (Lewis and von Elbe, 1987).
However, measurement is a difficult task since the data of the minimum ignition energy strongly scatter depending on the material shape of the electrodes, the properties of the electric discharge, the spark duration (Zhang et al., 2012), the initial pressure and temperature and the pre-ignition turbulence level (Pan et al., 2022, 2021).
In the chemical industry, a certain level of pre-ignition turbulence can occur either unintentionally (as in the case of dust cloud formation caused by a blast of air investing a dust deposit in a process unit) or intentionally. Indeed, turbulent combustion is of fundamental and practical importance. For example, turbulent premixed combustion combined with high compression ratios has a great potential to increase fuel consumption and reduce NOx emissions in petrol engines (Heywood, 1988).
Methane is one of the most studied fuels, since it occurs as a major component of natural gas or mine gas. Measurements of its flammability limits in air or other oxidants, critical energy for explosion initiation (in deflagration or detonation mode), and its dispersion characteristics under confined conditions are published regularly as experimental methods are updated and methane is increasingly used as a clean transportation fuel. Methane combustion in internal combustion engines produces fewer pollutants than gasoline, diesel fuel, or propane/LPG fuels. CNG (compressed natural gas) is used in conventional gasoline/combustion engine vehicles that have been converted or manufactured to run on CNG, either alone, with a separate gasoline

Paper Received: 9 April 2023; Revised: 11 June 2023; Accepted: 25 August 2023
Please cite this article as: Portarapillo M., Di Benedetto A., 2023, Turbulent Ignition Regimes in 20 L Explosion Vessel: CFD Simulations, Chemical Engineering Transactions, 104, 67-72 DOI:10.3303/CET23104012

system to increase range (dual-fuel engines), or in conjunction with another fuel such as diesel (bi-fuel engines) (Mitu et al., 2017).
The present work fits into this scenario, where understanding the interaction between the ignition source and the degree of pre-ignition turbulence is of paramount importance for both accident prevention and internal combustion engine operation. For this purpose, we performed CFD simulations of unsteady premixed flame propagation during explosion of stoichiometric homogeneous CH_4/air in a closed spherical vessel. Simulations were run by setting different preignition turbulence levels and ignition energies. The energy source is generated by means of spark ignition models or by using hot cores of different size where the progress variable is equal to the unity (burned products). The Peters model was chosen as combustion sub-model.
The main objective of the work is to provide a general operating map, identifying the ignition regimes as a function of the pre-ignition turbulence level present in the vessel, highlighting the non-ignition and no-propagation energy values for each turbulence level.

2. Methodology

The computational domain and mesh of a 20 L sphere were built and refined by means of the Design Modeler and Meshing packages of Ansys (Release 22). The sphere was modeled as three-dimensional. The model solves the unsteady time-averaged Navier-Stokes (URANS) equations expressing the conservation of mass, momentum, energy, and chemical species. The URANS equations were solved using the k-ε standard model as a turbulent sub-model with standard wall function and considering compressibility effects (Launder and Spalding, 1972). The flow equations were discretized using a finite volume formulation on the three-dimensional non-uniform unstructured grid (176072 elements, elements maximum size 0.0126 m, elements minimum size 0.00136 m), whose convergence was opportunely verified (Figure 1a). The semi-implicit method for pressure-coupled equations (SIMPLE) was used to solve the equations with pressure-velocity coupling. First-order schemes for convective terms and second-order schemes for diffusion terms were used in the spatial discretization of the model equations. First-order temporal integration was used to discretize the time derivatives with a time step of $4\text{-}10^{-5}$ s. To model the premixed combustion of the stoichiometric CH_4/air mixture, the equation for species transport was reformulated in terms of a transport equation for the reaction progress variable c:

$$\frac{\partial(\rho c)}{\partial t} + \boldsymbol{\nabla} \cdot (\rho \boldsymbol{u} c) = \boldsymbol{\nabla} \cdot \left(\frac{\mu_t}{Sc_t} \boldsymbol{\nabla} c\right) + \rho S_c \qquad (1)$$

Where ρ (kg/m^3) is the gas density, c (-) is the mean reaction progress variable (c=0 unburnt mixture, c=1 burnt mixture), $\boldsymbol{u}$ (m/s) is the vectorial velocity of the mixture, μ_t (kg/(ms)) is the turbulent viscosity of the mixture, Sc_t (-) is the turbulent Schmidt number and S_c (1/s) is the reaction progress source term. The Peters model was chosen as combustion sub-model to close S_c (Peters, 2001). For the simulated stoichiometric CH_4/air flame, the laminar combustion velocity was assumed to be constant with pressure and temperature and equal to 0.35 m/s. The specific heat values of the unburned and burned mixtures were calculated as piecewise polynomial functions of the fifth power of temperature. The molecular viscosities were calculated according to Sutherland's law for air viscosity. In the simulations, different ignition energies were simulated by placing hot hearts at 2000 K and progress variable equal to 1 (burnt gases) in the center of the sphere, characterized by different radius values as a function of energy (Figure 1b).

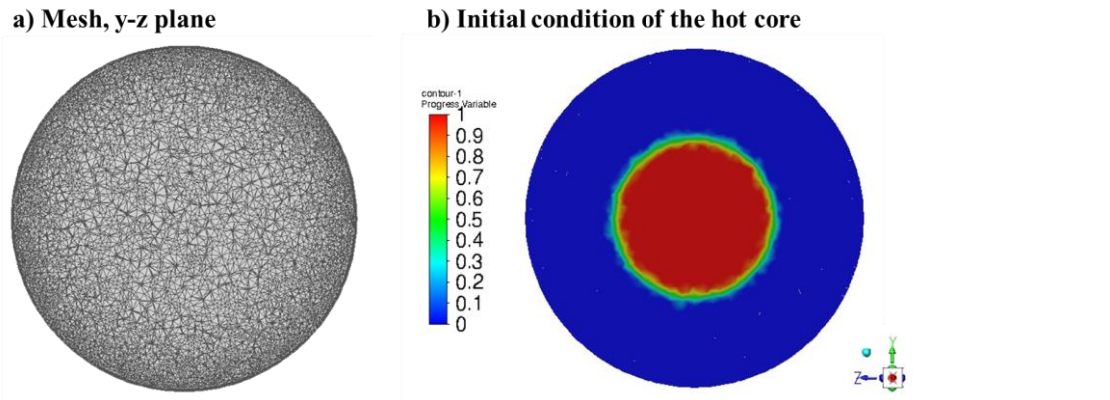

Figure 1: Mesh (a) and initial condition in terms of progress variable in the case of 500 J ignition energy.

The radius was determined in previous work using Dahoe's thin flame model applied to experimental tests in a 20 L sphere with varying ignition source (Dahoe et al., 1996; Portarapillo et al., 2021a, 2021b) and also used in the case of 1 m^3 vessel (Portarapillo et al., 2022, 2021c). The ignition energies considered are well above the minimum ignition energy of the stoichiometric methane-air mixture (White et al., 2006) and are the typical ones used in the 20 L sphere for the combustible dust characterization test. This choice was made to demonstrate the effective interaction of the ignition source with the turbulence even in the presence of extreme overdrive of the gas mixture. The evolution of the trigger radius as a function of energy level is shown in Figure 2.

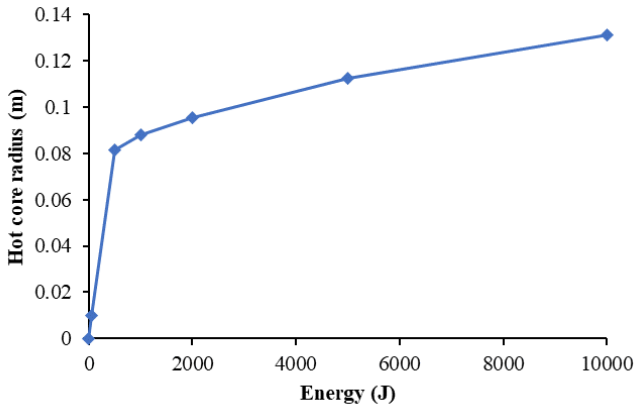

Figure 2: Trend of the hot core radius as a function if the ignition energy level as assessed in a previous work (Portarapillo et al., 2021a).

In addition to the initial condition related to the triggering source, the level of pre-ignition turbulence was changed for each energy level. In particular, a certain value of turbulent kinetic energy *k* that was set within the whole domain, and the corresponding turbulent kinetic energy dissipation rate *ε* value was evaluated with the following equation (Peters, 2001):

$$\varepsilon = \frac{k^{3/2}}{R} \quad (2)$$

Where R (m) is the vessel radius i.e., the maximum size of the turbulent vortices.
All initial conditions of the simulation in terms of ignition energy (and associated hot core radius), turbulent kinetic energy, and turbulent kinetic energy dissipation rate are listed in Table 1.

Table 1: Summary of the investigated initial conditions

Hot core radius (m)	Corresponding ignition energy (J)	Turbulent kinetic energy (m^2/s^2)	Turbulent kinetic energy dissipation rate (m^2/s^3)
0.006	10 (Spark ignition)	15	342
		50	2080
		100	5882
0.01	50	15	342
		50	2080
		100	5882
		200	16237
0.08	500	15	342
		50	2080
		100	5882
		200	16237
0.087	1000	15	342
		50	2080
		100	5882
		200	16237

3. Results

Figure 3 shows the results of the simulations performed in terms of the pressure profile as a function of time, varying the level of pre-ignition turbulence and the ignition energy. In general, when ignition occurs, the trends are in agreement with that obtained by Di Benedetto et al. (2016) (Di Benedetto and Di Sarli, 2016).
As can be seen from Figures 3c and 3d, in the case of 500 and 1000 J (maximum overdrive of the mixture), the pressure profile always reaches a plateau corresponding to the complete combustion of the stoichiometric mixture and the attainment of the maximum pressure under adiabatic conditions. This means that when very intense ignition sources are used, very strong turbulence cannot dissipate the hot core, so that complete consumption of the mixture is achieved. On the contrary, it can be seen in Figure 3a that at the weakest triggering energy, the effect of pre-ignition turbulence is important. In particular, above a turbulent kinetic energy of 15 m^2/s^2, the triggering source of 10 J is dissipated precisely because of the turbulence. The same behavior is observed at an energy of 50 J (Figure 1b), but at a higher turbulence level.
The failure of flame propagation can be explained using Figure 4. Particularly, Figure 4 shows the maps of the progress variables, turbulent kinetic energy, and pressure after reaching the pressure plateau in the case of a 50 J ignition with k=15 m^2/s^2 and k=200 m^2/s^2. In the case of a lower turbulence level (Figure 4a), ignition is not affected in the first moments and flame propagation continues successfully, leading to a complete consumption of the gas mixture (c=1), the achievement of a high post-combustion turbulence and the adiabatic pressure. At the strongest turbulence (Figure 4b), ignition occurs and the ignition kernel is generated, but it affects the gas mixture only in the regions immediately adjacent to the hot core. After that, the propagation can no longer be sustained, and the high turbulence level promotes the homogenization of all variables involved.
As can be seen in Figure 3c and 3d, before reaching the plateau, the pressure exhibits strong oscillations which gradually become more intense as the pre-ignition turbulence increases. Notably, at these ignition energy, the gaseous mixture at the initial condition is completely burnt as the hot core occupies most of the sphere. After a few moments (already at 5E-4 s), the mixture is totally burned, generating an intense pressure wave accompanied by a high turbulence which hits the walls and goes back, compressing the mixture also in the center of the vessel. This behavior is also verified by the analysis of the velocity vectors (not shown).

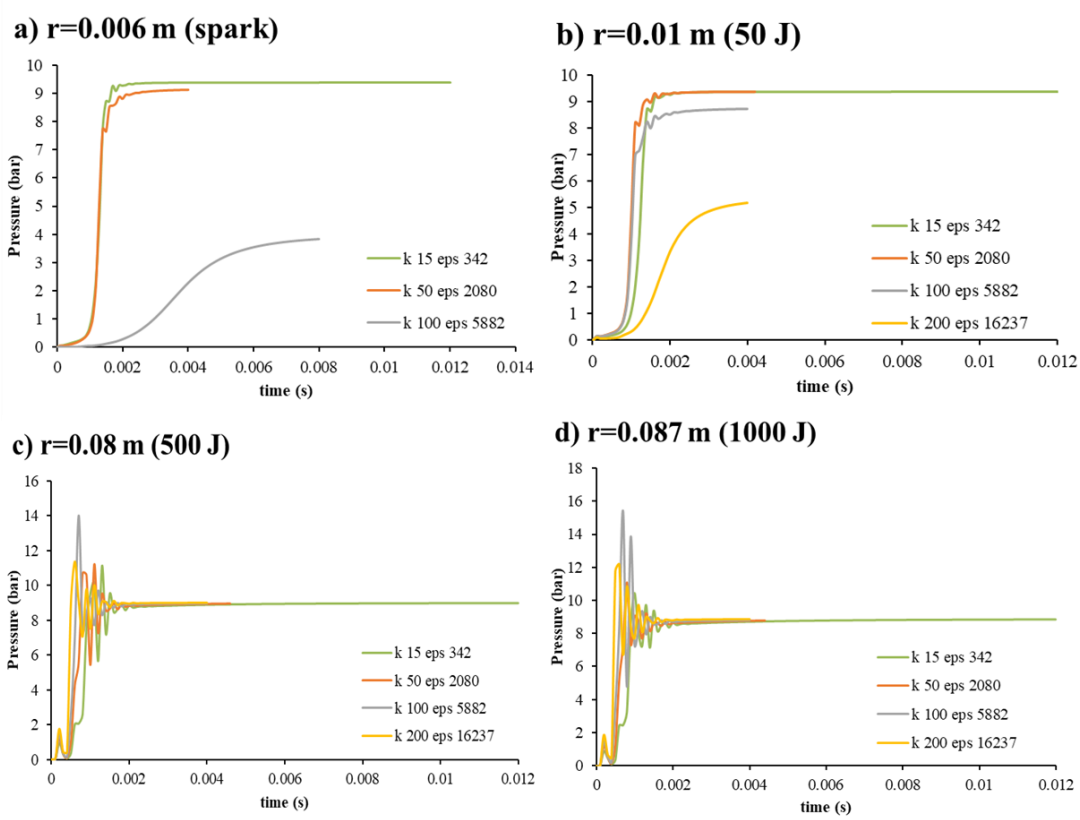

Figure 3: Pressure profiles as functions of time, varying the level of pre-ignition turbulence and the ignition energy.

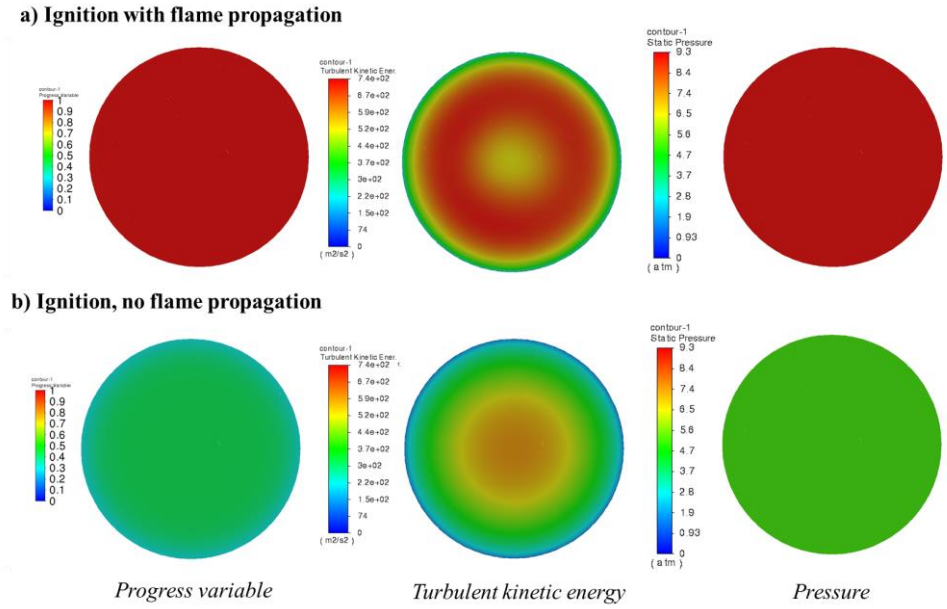

Figure 4: Maps of the progress variables, turbulent kinetic energy, and pressure after reaching the pressure plateau in the case of a 50 J ignition with k=15 m^2/s^2 (a) and k=200 m^2/s^2 (b).

To summarize the results obtained, an operational map of ignition energy as a function of turbulent kinetic energy was constructed. Figure 5 shows such a map. In particular, for turbulent kinetic energies greater than 500 m^2/s^2 (simulation not shown), no ignition energy, no matter how strong, succeeds in ensuring subsequent flame propagation. For lower turbulence values, the curve in the figure describes the division of the zone into a flame propagation zone (white zone) and a non-propagation zone (blue one).
Limit conditions reported on the curve can be evaluated by regression:

$$IE_{prop} = 0.0038k^2 + 0.0949 \quad (3)$$

Where IE_{prop} (J) is the ignition energy limit at a given turbulence level below which no flame propagation occurs, but above which ignition and propagation occurs.

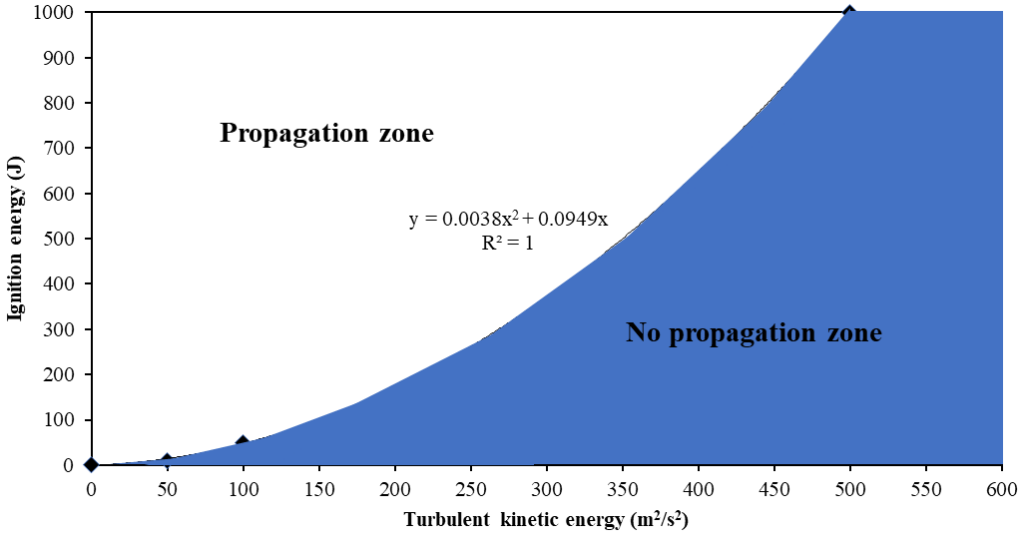

Figure 5: Operational map in terms of ignition energy and turbulent kinetic energy for the stoichiometric methane-air mixture.

4. Conclusions

In this work, CFD simulations of ignition and flame propagation have been performed in a perfectly premixed methane-air stoichiometric mixture. Many simulations have been carried out by varying the ignition energy and the pre-ignition turbulence level. In particular, to simulate different ignition energies, hot cores at 2000 K of different radius were created and for the variation of the turbulence, the turbulent kinetic energy and its dissipation rate were modified.

Through the evaluation of the pressure trends and of the progress variable and pressure map, it was possible to discriminate the cases in which the flame propagation occurred from those in which the turbulence is so intense as to cause the fragmentation of the ignition kernel and the homogenization of all the variables involved. In the event of flame propagation failure, the mixture present inside the vessel does not react completely, showing a progress variable other than 1 at the pressure plateau which in this case is not equivalent to the adiabatic one.

In order to provide a simple predictive tool to evaluate the presence of flame propagation, given the turbulence conditions, an operational map has been constructed in which the flame propagation and non-propagation zones are visible. From this, the boundary conditions are highlighted and can be calculated by means of a simple regression. this tool is valid for the methane-air stoichiometric mixture (identified in the model with its laminar flame velocity) and can be useful both for technological purposes in the field of combustion but also for safety purposes. In particular, this approach can be coupled with CFD-based risk analysis of gaseous substance releases to have an assessment of the local ignition probability once the turbulent flow field is known, especially in confined conditions.

References

Dahoe A.E., Zevenbergen J.F., Lemkowitz S.M., Scarlett B., 1996, Dust explosions in spherical vessels: The role of flame thickness in the validity of the “cube-root law.” J. Loss Prev. Process Ind., 9, 33–44.

Di Benedetto A., Di Sarli V., 2016, The role of turbulence in the validity of the cubic relationship. J. Loss Prev. Process Ind., 43, 593–599.

Heywood J.B., 1988, Internal Combustion Engine Fundamentals. McGraw-Hill, New York.

Launder B.E., Spalding D.B., 1972, Lectures in mathematical models of turbulence. Academic Press, London; New York.

Lewis B., von Elbe G., 1987, Combustion, Flame and Explosions of Gases. Academic Press, London.

Mitu M., Giurcan V., Razus D., Prodan M., Oancea D., 2017. Propagation indices of methane-air explosions in closed vessels. J. Loss Prev. Process Ind., 47, 110–119.

Pan J., He Y., Wang L., Li T., Wei H., Shu G., 2022, Effects of thermal stratification and turbulent intensity on auto-ignition and combustion mode transition. Combust. Flame, 244.

Pan J., Zheng Z., Wei H., Pan M., Shu G., Liang X., 2021, An experimental investigation on pre-ignition phenomena: Emphasis on the role of turbulence. Proc. Combust. Inst., 38, 5801–5810.

Peters N., 2001, Turbulent Combustion. Meas. Sci. Technol., 12, 2022.

Portarapillo M., Sanchirico R., Di Benedetto A., 2021a, On the pyrotechnic ignitors role in dust explosion testing : Comparison between 20 L and 1 m 3 explosion vessels, Process Saf. Prog., 40, 289–295.

Portarapillo M., Sanchirico R., Di Benedetto A., 2021b, Effect of turbulence spatial distribution on the deflagration index: Comparison between 20 L and 1 m3 vessels, J. Loss Prev. Process Ind., 71, 104484.

Portarapillo M., Trofa M., Sanchirico R., Di Benedetto A., 2022, CFD simulation of turbulent fluid flow and dust dispersion in the 1 m3 explosion Vessel equipped with the rebound nozzle, J. Loss Prev. Process Ind., 76, 104755.

Portarapillo M., Trofa M., Sanchirico R., Di Benedetto A., 2021c, CFD simulations of the effect of dust diameter on the dispersion in the 1 m3 explosion vessel, Chem. Eng. Trans., 86, 343-348.

White C.M., Steeper R.R., Lutz A.E., 2006, The hydrogen-fueled internal combustion engine: a technical review, Int. J. Hydrogen Energy, 31, 1292–1305.

Zhang Q., Li W., Liang H.M., 2012, Effect of spark duration on explosion parameters of methane/air mixtures in closed vessels, Saf. Sci., 50, 1715–1721.